5th North American Particle Accel. Conf. NAPAC2022, Albuquerque, NM, USA JACoW Publishing
ISBN: 978-3-95450-232-5 ISSN: 2673-7000 doi:10.18429/JACoW-NAPAC2022-TUZE6

STUDIES OF ION INSTABILITY USING A GAS INJECTION SYSTEM*

J. Calvey, M. Borland, L. Emery, P.S. Kallakuri, ANL, Argonne, IL 60439, USA

Abstract

Residual gas ions can cause a variety of undesirable effects in electron storage rings, including coherent instability and incoherent emittance growth. This is a serious concern in next-generation light sources due to challenging emittance and stability requirements. A gas injection system was designed and installed in the present APS ring to study such effects using a controlled pressure bump. Measurements were taken under a wide variety of beam conditions, using a spectrum analyzer, pinhole camera, and bunch-by-bunch feedback system. The feedback system was also used to perform grow-damp measurements, allowing us to measure the growth rate of individual unstable modes. This paper presents some of the results of these experiments, along with simulations using the tracking code `elegant`.

INTRODUCTION

The APS-Upgrade is a 4th-generation light source currently under development at Argonne National Laboratory [1], with a design emittance of 42 pm at 6 GeV. In order to make use of this ultra-low emittance, potential instabilities must be anticipated and mitigated.

Ion instability is of particular concern. Trapped ions can produce a fast-growing transverse (usually vertical) instability, due to coupled motion of the beam and ions. Simulations predict a strong coherent ion instability for 324 bunch mode, which we plan to mitigate with a compensated gap scheme [2]. Additionally, incoherent effects such as emittance growth may still be an issue even if the coherent instability is damped.

To better understand the ion instability and anticipate issues in the APS-U storage ring, we installed a gas injection system in an empty insertion device (ID) straight section in Sector 25 (S25) of the present APS storage ring. This enabled us to create a controlled and localized pressure bump, and study the resulting instability. The system was later relocated to Sector 35 (S35). The lattice functions are quite different at the two locations, which allows for some interesting comparisons.

EXPERIMENTAL SETUP

The gas-injection system is described in detail in Ref. [3]. It allows creation of a controlled pressure bump of either 100 nTorr or 900 nTorr of N_2. The ion pump located next to the gas injection location is disabled for the study, while ion pumps upstream and downstream of the injection point are kept on to localize the bump. Measurements showed that the bump was mostly localized to a ~6 m section in Sector 25, and a ~10 m section in Sector 35.

Figure 1 compares two relevant parameters at the two gas injection locations, over the approximate area of the pressure bumps. The first is the critical mass [4]; a lower critical mass will result in more ion trapping. The second parameter, $\tau_y \equiv 10^{10}\,\sigma_y(\sigma_x+\sigma_y)/\beta_y$ is proportional to the vertical instability growth time. A lower τ_y indicates a faster growing instability (at least initially).

At S25, A_{crit} and τ_y are highly correlated, meaning that locations with the most trapping have the highest growth rate. At S35, they are almost anti-correlated, so the locations with more trapping tend to have lower growth rates. Overall, both the critical mass and growth time are lower at S35, so the vertical instability should be stronger there.

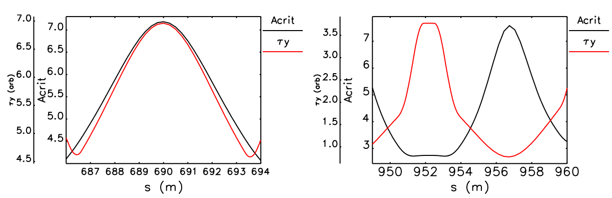

Figure 1: Critical mass and vertical instability growth times at S25 (left) and S35 (right). The gas injection point is at 690 m for S25, and 954.5 m for S35.

TRAIN GAP STUDIES

Several experiments were performed with this system, under a wide variety of beam conditions. Measurements were taken with a pinhole camera, spectrum analyzer, and Dimtel feedback system [5]. Where possible, measurements taken during the S25 experiment were repeated at S35. For one such study, we examined the effect of different train gaps on the instability. Four different bunch patterns were used: 1 train with no gaps, 4 trains with a 12 bunch gap in between them ("12bg"), 4 trains with 24 bunch gaps ("24bg"), and 4 trains with 12 bunch gaps and 6 double-charge guard bunches before and after the gap ("12bg 6gb"). A similar guard bunch scheme will be used at APS-U, to minimize rf transients and provide a stronger kick to the ions before the gap [2].

Basic ring and beam parameters for these experiments are given in Table 1. All measurements shown in this paper used the 900 nTorr pressure bump. With the 100 nTorr bump, only the no gap case had significant instability.

Table 2 lists emittances measured with the pinhole camera for both S25 and S35 experiments. For S25 with no gaps, there is a large blowup of both emittances. The horizontal blowup is mitigated by any type of gap (ϵ_x is slightly higher for all S25 cases, mostly likely due to a measurement error). For S35 without gaps, the vertical blowup is an order of

* Work supported by the U.S. Department of Energy, Office of Science, Office of Basic Energy Sciences, under Contract No. DE-AC02-06CH11357.

ISBN: 978-3-95450-232-5 ISSN: 2673-7000 doi:10.18429/JACoW-NAPAC2022-TUZE6

Table 1: APS Storage Ring Parameters for the Gas Injection Experiments

Quantity	Value
Beam energy	6 GeV
Horizontal, vertical emittance	1.83 nm, 24 pm
Revolution time	3.68 μs
Beam current	~80 mA
Bunches (no gaps)	324
Bunch spacing	11 ns
horizontal,vertical chromaticity	~6,~3

magnitude larger (as predicted above), while the horizontal blowup is modest. For both locations, a 12-bunch gap reduces the effect, but does not eliminate it. A 12-bunch gap with guard bunches performs better than 12-bunch gap without them, and roughly the same as a 24-bunch gap.

Table 2: Measured Emittances with the 900 nTorr Bump (Cases with Large Blowup are Shown in Bold)

Pattern	S25 ϵ_x (nm)	S35 ϵ_x (nm)	S25 ϵ_y (nm)	S35 ϵ_y (nm)
No gap	**3.6**	1.98	**0.124**	**1.55**
12bg	2.06	1.83	0.049	**0.188**
12bg 6gb	2.05	1.78	0.031	0.043
24bg	2.09	1.77	0.027	0.051

One signature of ion instability is elevation of lower vertical betatron sidebands near a characteristic frequency, expected to be ~11 MHz for S25 and ~8 MHz for S35. Figure 2 shows a measurement of these sidebands. As expected, the S35 results show a much larger amplitude and lower ion frequency than the S25 results. In both locations, with no gaps, the instability is very strong and the ion frequency is lower than expected. This indicates beam size blowup, since the frequency is inversely proportional to the beam size. Using train gaps reduces the instability amplitude and increases the ion frequency. The guard bunch case shows reduced instability compared to a 12 bunch gap without guard bunches, but slightly more than the 24 bunch gap.

Figure 3 shows the rms bunch positions over 9000 turns for the four S35 cases, as measured with the Dimtel system. One can see the instability build up over a single bunch train, indicating a "fast ion" instability [6]. Notably, the first few bunches in each train are more unstable than the immediately following bunches. The effectiveness of train gaps is apparent.

TRANSVERSE FEEDBACK

The Dimtel system is used to measure and suppress transverse instabilities. It detects the turn-to-turn bunch centroid deviation of individual bunches and calculates/applies correction kicks. As shown in Fig. 4, the vertical plane feedback was extremely effective, even for the most severe instability (900 nTorr, no gaps). However, the suppression of the vertical instability leads to a (smaller, but still significant) instability in the horizontal plane. One potential explanation for this effect is as follows: as the instability is suppressed in one plane, the clearing effect from beam shaking in that plane is reduced. This allows the ion density to increase, which causes a stronger instability in the other plane. With feedback on in both planes, this horizontal instability can be greatly reduced, but not totally eliminated.

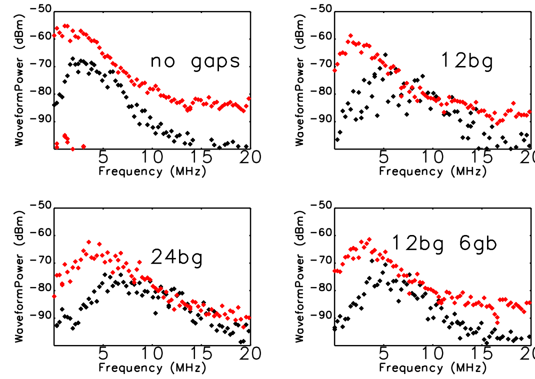

Figure 2: Vertical beam spectrum for different types of train gaps, 900 nTorr, for both the S25 (black) and S35 (red) experiments.

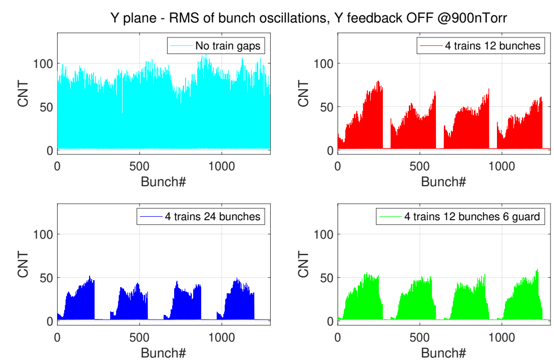

Figure 3: RMS motion of each bunch (over 9000 turns), S35, for each of the four cases.

Besides the feedback function, the system also has diagnostic capabilities such as grow/damp measurements to analyze unstable modes. The feedback on/off interval is modulated and bunch oscillation envelopes in are measured in the time domain. Evolution of unstable mode amplitudes over multiple tuns is computed using measured bunch data.

Figure 5 shows grow-damp measurements for each of the four train gap cases listed above. Feedback is disabled at 0 ms, and re-enabled at 20 ms. The instability grows very quickly, and is mostly saturated by ~10 ms. Even after saturation, the mode amplitudes are not constant. Rather, there is sharing of the instability between the modes. Note that these modes cover roughly the same frequency range as the spectrum analyzer plots above.

Grow-damp measurements allow quantifying the instability on a mode-by-mode basis. The initial growth and

5th North American Particle Accel. Conf. NAPAC2022, Albuquerque, NM, USA JACoW Publishing
ISBN: 978-3-95450-232-5 ISSN: 2673-7000 doi:10.18429/JACoW-NAPAC2022-TUZE6

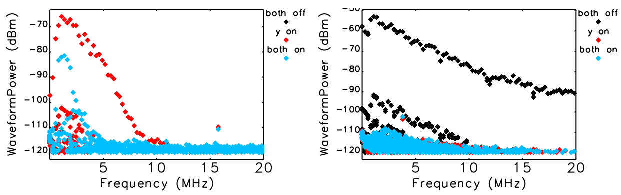

Figure 4: Spectrum analyzer measurements, comparing vertical feedback on and off, 900 nTorr, S35. Left: horizontal beam spectrum. Right: vertical spectrum. With feedback off in both planes, there is no measurable horizontal instability.

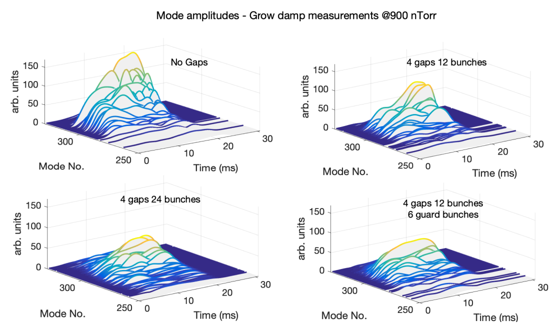

Figure 5: Grow-damp measurements, for each of the four cases, S35, 900 nTorr.

saturation can be modeled by a generalized logistic function, $y(t) = \alpha/(1+e^{-rt})^{1/\delta}$. Here α gives the saturation level of the mode, while r and δ define the shape of the curve. We can characterize the instability growth with the inflection point time $t_i \equiv -\ln(\delta)/r$. These parameters for four modes taken from a no gap measurement (Fig. 5, top left) are given in Table 3. Interestingly, modes with higher saturation levels have higher inflection times, i.e., stronger modes grow more slowly. This is consistent with Fig. 1 (right), which shows that the critical mass and growth time are anti-correlated at S35. Thus the modes with the highest amplitude are driven by locations with the most ion trapping, rather than those with the fastest initial growth.

Table 3: Logistic Fit Parameters

mode	freq (MHz)	α	t_i (ms)
301	6.2	24.6	3.9
308	4.3	34.4	4.1
317	1.9	98.6	11.1
320	1.1	148.5	17.0

SIMULATIONS

Simulations using the IONEFFECTS element in the tracking code elegant [7,8] were performed for each of the train gap cases. The simulations include transverse impedance, multiple ionization, and use the actual measured bunch patterns [9]. The bi-Gaussian method [10] is used for modeling ion-beam kicks. Simulations using the single Gaussian method underestimated the instability in most cases.

Figure 6 shows simulation results for S35, at 900 nTorr. The left plot gives the ion density vs time for the first few turns. The clearing effect from the train gaps is readily seen. For the cases with gaps (especially 24bg), the ion density does not always grow monotonically along the bunch train; rather there is a dip in the middle. This may be related to the non-monotonic instability growth seen in Fig. 3.

Figure 6 (right) gives the effective emittance vs time. This is obtained by adding the beam size and rms bunch motion in quadrature, and is roughly what is measured by the pinhole camera. The simulations show a very strong and fast-growing instability for the no gap case. The cases with gaps show a slower but non-negligible blowup in the effective emittance. Compared to the measurements (Table 2), the simulations tend to overestimate the emittance blowup, by as much as a factor of 2. There is qualitative agreement on two key points: any type of gap drastically reduces the instability, and the guard bunch case performs significantly better than the case without guard bunches.

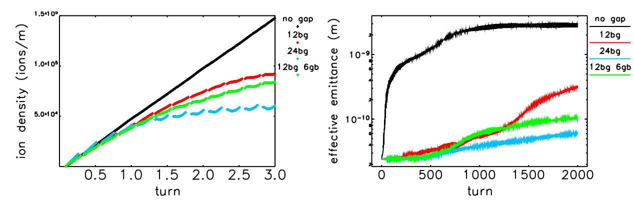

Figure 6: IONEFFECTS simulations of the four cases, S35. Left: ion density for the first three turns. Right: effective emittance for 2000 turns (note the log scale.)

CONCLUSIONS

A gas injection system has been installed and used to study ion instability, at two different locations in the APS ring. Train gap studies have demonstrated that gaps are effective at mitigating the instability, and that guard bunches help with the ion clearing. Experiments with a bunch-by-bunch transverse feedback system have demonstrated that the feedback can effectively damp the instability in both planes simultaneously. The system has also been used to perform grow-damp measurements, and study the growth of the instability on a mode-by-mode basis.

IONEFFECTS simulations using a bi-Gaussian kick method show qualitative agreement with the measurements, though they tend to overestimate the instability amplitude. Work is underway to implement a Poisson solver in the code. Simulations using a model of the transverse feedback will also be performed.

ACKNOWLEDGMENTS

We would like to thank the APS vacuum group, especially J. Hoyt, for building and operating the gas injection system. We gratefully acknowledge the computing resources provided on Bebop, a high-performance computing cluster operated by the Laboratory Computing Resource Center at Argonne National Laboratory.

ISBN: 978-3-95450-232-5 ISSN: 2673-7000 doi:10.18429/JACoW-NAPAC2022-TUZE6

REFERENCES

[1] R. O. Hettel, "Status of the APS-U Project", in *Proc. IPAC'21*, Campinas, Brazil, May 2021, pp. 7–12. doi:10.18429/JACoW-IPAC2021-MOXA02

[2] J. Calvey and M. Borland, "Modeling Ion Effects for the Argonne Advanced Photon Source Upgrade", *Phys. Rev. Accel. Beams*, vol. 22, no. 11, p. 114403, 2019. doi:10.1103/PhysRevAccelBeams.22.114403

[3] J. R. Calvey *et al.*, "Measurements of Ion Instability and Emittance Growth for the APS-Upgrade", in *Proc. IBIC'20*, Santos, Brazil, Sep. 2020, pp. 258–262. doi:10.18429/JACoW-IBIC2020-THPP25

[4] H.G. Hereward, "Coherent Instability due to Electrons in a Coasting Proton Beam", CERN, Geneva, Switzerland, Rep. CERN-71-15, Jul. 1971.

[5] Dimtel iGp12 product details, https://www.dimtel.com/products/igp12

[6] J. Byrd *et al.*, "First Observations of a Fast Beam-Ion Instability", *Phys. Rev. Lett.*, vol. 79, no. 1, pp. 79–82, 1997. doi:10.1103/PhysRevLett.79.79

[7] M. Borland, "elegant: A Flexible SDDS-Compliant Code for Accelerator Simulation", Rep. LS-287, APS, Sep. 2000.

[8] Y. Wang and M. Borland, "Pelegant: A Parallel Accelerator Simulation Code for Electron Generation and Tracking", in *Proc. AAC 2006*, vol. 877, p. 241, 2006.

[9] J. Calvey and M. Borland, "Simulation of Incoherent Ion Effects in Electron Storage Rings", *Phys. Rev. Accel. Beams*, vol. 24, no. 12, p. 124401, 2021. doi.org/10.1103/PhysRevAccelBeams.24.124401

[10] J. R. Calvey *et al.*, "Advances in Understanding of Ion Effects in Electron Storage Rings", in *Proc. IPAC'21*, Campinas, Brazil, May 2021, pp. 1267–1272. doi:10.18429/JACoW-IPAC2021-TUXA01